Carbohydrate Polymers 98 (2013) 1065–1071

Contents lists available at SciVerse ScienceDirect

Carbohydrate Polymers

journal homepage: www.elsevier.com/locate/carbpol

Assessment of the changes in the cellulosic surface of micro and nano banana fibres due to saponin treatment

Nereida Cordeiro[a,*], Marisa Faria[a], Eldho Abraham[b], Laly A. Pothan[b]

[a] Competence Centre in Exact Science and Engineering, University of Madeira, 9000-390 Funchal, Portugal
[b] Post Graduate Department of Chemistry, Bishop Moore College, Mavelikara, 690110, Kerala, India

ARTICLE INFO

Article history:
Received 3 December 2012
Received in revised form 4 June 2013
Accepted 3 July 2013
Available online 12 July 2013

Keywords:
Saponin treatment
Surface properties
Celulose
Banana fibres
Inverse Gas Chromatography

ABSTRACT

The effect of saponin on the surface properties of banana fibres was studied by Inverse Gas Chromatography (IGC). Parameters including the dispersive component of the surface energy, surface heterogeneity, surface area, as well as acid–base surface properties were determined for saponin modified banana micro and nanofibres. These parameters show a more extensive saponin coating on the nanofibres with a network formation which is explained by the higher reactivity of nanofibres due to the higher surface energy, specific interaction and higher surface area presented by the nanofibres. The energetic profile indicates that both micro and nanofibres coated with saponin interact with the same, or similar, energy active sites. Saponin treatment reduces considerably the surface area of the fibres, with the consequent decrease in the monolayer capacity. The interaction with the polar probes clearly indicates that saponin treatment creates new polar active sites for specific interactions in both samples. However, the treatment increases predominately the basicity of the fibre surface with more relevance to the nanofibres. This behaviour will lead to better polymer/fibre interaction during composite preparation.

1. Introduction

In nature, a large number of plants and animals synthesize extra-cellular high-performance skeletal biocomposites consisting of a matrix reinforced by fibrous biopolymers (Mohanty, Misra, & Hinrichsen, 2000). Cellulose is a classic example where the reinforcing elements exist as whisker-like microfibrils that are biosynthesized and deposited in a continuous manner. The promising performance of cellulose fibres and their abundance encourages the utilization of agricultural waste residue, which acts as the main source of cellulose. Natural fibres are an environmental friendly alternative to glass fibres used in traditional commercial composite materials (Mohanty et al., 2000; Eichhorn et al., 2001). Cellulosic fibres offer great opportunities to develop new ecologically adaptable light weight structural composites due to its appealing properties, such as low density, biodegradability, recyclability, renewability and low cost (Lu, Askeland, & Drzal, 2008).

Banana fibre obtained from the pseudo stem of banana plant is one of the major underutilized raw material in tropical and sub-tropical regions which is composed by 70% of cellulose in dry weight (Oliveira, Cordeiro, Evtuguin, Torres, & Silvestre, 2007). Recently, Abraham et al. (2011) have reported the preparation of nanocellulose from banana fibres by steam explosion. This fractionation treatment allows the modification of physical properties with the breakdown of biomass components by steam heating. The obtained nanocellulose can be used as an excellent reinforcing agent in biodegradable polymer systems due to its high surface area, unique morphology and mechanical strength (Habibi, Lucia, & Rojas, 2010).

Although cellulosic fibres have a great industrial utility, its properties can be enhanced with chemical modification. Chemical surface modification can improve the cellulosic fibres compatibility and efficiency in polymer systems. Modified biomaterials can maintain the intrinsic mechanical properties while improving the tissue biocompatibility. Therefore, improved biomaterials can be controlled by chemically modifying their bio-interaction properties, such as adhesion, polarity and reactivity.

Surface modification chemical agents are widely used surface-active substances, also known as surfactants. Saponins are a group of secondary metabolites present in over 500 species (Guglu-Ustundag & Mazza, 2007). *Sapindus mukorossi* (Sapindaceae), better known as "soapnut tree", is an economically important agricultural plant in tropical and sub-tropical regions of Asia as a source of natural surfactants (Rao, Basa, & Srinivasulu, 1992). Saponin molecules have various complex organic structures which present amphiphilic characteristics generated from lipophilic and hydrophilic sites present in their structures (Böttger, Hofmann, & Melzig, 2012). Saponins are composed by saccharides residues (polar) attached to a triterpenoid or steroid backbone

* Corresponding author. Tel.: +351 291 705 107; fax: +351 291 705 149.
E-mail address: ncordeiro@uma.pt (N. Cordeiro).

0144-8617/$ – see front matter © 2013 Elsevier Ltd. All rights reserved.
http://dx.doi.org/10.1016/j.carbpol.2013.07.002

(apolar) by glycosidic linkage, providing saponins with strong surface-active properties (Böttger et al., 2012). This structure gives saponin molecules the ability to interact with hydrophilic and hydrophobic sites of other molecules. The main reactive side group of the saponin can be summarized as chromosaponin (Tsurumi et al., 2000):

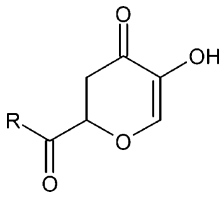

The improvement of biomaterials requires a careful characterization of the modified surface structure. Inverse Gas Chromatography (IGC) is now a well-established technique for the determination of the surface properties, including London (i.e. apolar) and specific (i.e. polar) interactions, at the molecular level. The flexibility of IGC technique makes it a valid tool in the characterization of various materials. In recent years, IGC has been used to characterize and optimize the interaction of natural fibres and polymer composites (Tze, Wålinder, & Gardner, 2006; Belgacem et al., 2011; Cordeiro, Gouveia, & John, 2011; Cordeiro, Mendonça, Pothan, & Varma, 2012).

In the present study, IGC was used to study the effect of saponin treatment onto the surface of micro and nano banana fibres. The surface characteristics were evaluated and co-related to the changes occurring during the chemical modification.

2. Materials and methods

2.1. Materials

Pseudo-stem banana fibres (*Musa sapientum*) were collected from Marthandom, Tamil Nadu, India. This fibre (banana microfibres) was subjected to steam explosion coupled with basic and acid treatment as described by Cherian et al. (2008). The acid hydrolysed banana fibres treated with 11 wt% oxalic acid were used in this work (banana nanofibres).

For the IGC experimentals, the *n*-alkane probes were: *n*-hexane (C_6), *n*-heptane (C_7), *n*-octane (C_8), *n*-nonane (C_9) and *n*-decane (C_{10}). The polar probes were: tetrahydrofuran, ethyl acetate, ethanol and acetonitrile; all GC grade (>99% of purity) supplied by Sigma-Aldrich. The methane, used as a non-interacting reference probe, and the carrier gas, helium, were of high purity (>99.99%) and were supplied by Air Liquid Company.

2.2. Surface treatment

Soapnuts were obtained from the tree of *S. mukorossi* which is widely distributed in the southern parts of India. The soapnut seed has an outer protective layer, leathery-skinned drupe with 1–2 cm in diameter, yellow ripening blackish, containing one to three seeds. This leathery-skinned drupe is used to extract the saponin. Dried leathery-skinned drupe was powdered by using a grinder.

The powder was stinging stirred with minimum amount of water and the foam formed on the surface of the water was collected and stored. The concentrated extract was made into a solution with ammonium sulphate (20 wt%). The fibres were treated under refluxing and kept at 80 °C for 3 h and again for another two weeks at room temperature to ensure the complete reaction between the fibres and the saponin extract. The ammonium sulphate was removed with filtration followed by repeated washing with distilled water. The absence of ammonium chloride was confirmed by adding lead chloride to the filtrate until it gives no precipitation of lead sulphate. After then, the modified samples were dried in an oven at 45 °C.

2.3. IGC measurement

IGC measurements were carried out on a commercial inverse gas chromatograph (*i*GC, Surface Measurement Systems, London, UK) equipped with a flame ionization (FID) and thermal conductivity (TCD) detector. The IGC system is fully automatic with SMS *i*GC Controller v1.8 control software. Standard glass silanized (dimethyldichlorosilane; Repelcote BDH, UK) columns with 0.4 cm ID and 30 cm in length were used.

About 1 g of the sample was packed in the columns by vertical tapping. The columns with the samples were placed in the IGC column oven module and conditioned over night at 333 K with helium at 10 ml/min of flow rate, in order to remove the impurities adsorbed on the surface. After conditioning, pulse injections were carried out with a 250 μl gas loop. After the probe molecule injection the adsorption followed by desorption takes place in the column sample. The interaction probe/sample cause retention, similar to analytical chromatography. In this study, the retention time was calculated from the FID response. The retention volume and subsequent data were analyzed using *i*GC Standard v1.3 and Advanced Analysis Software v1.21 based in the equations explained in the following section. The physical constants for probes used in IGC calculations were taken from the literature and are reported in Table 1.

Measurements of the dispersive interaction were made with the *n*-alkanes series at 293, 298 and 303 K. The carrier gas (helium) flow rate was 10 ml/min. To specific free energy studies, tetrahydrofuran, ethyl acetate, ethanol and acetonitrile were used at the same conditions. The permeability studies were done with *n*-octane at flow rate 3, 5, 7, 12, 17, 20, 24, 27, 31 and 34 ml/min. The isotherm experiment was undertaken with *n*-octane at 0.03, 0.04, 0.05, 0.08, 0.1, 0.3, 0.5, 0.7 and 0.9 p/p^0. Heat of sorption measurements was done with the n-alkanes and polar probes at

Table 1
Physical constants of the probes used in IGC experiments.

Probe	a (10^{-19} m^2)	γ_L^D (mJ/m^2)	DN (kcal/mol)	AN* (kcal/mol)	DN/AN*
n-Hexane	5.15	18.4	–	–	–
n-Heptane	5.73	20.3	–	–	–
n-Octane	6.30	21.3	–	–	–
n-Nonane	6.90	22.7	–	–	–
n-Decane	7.50	23.4	–	–	–
Ethanol	3.53	21.1	19.0	10.3	1.84
Acetonitrile	2.14	27.5	14.1	4.7	3.00
Acetone	3.40	16.5	17.0	2.5	6.80
Ethyl acetate	3.30	19.6	17.1	1.5	11.4
Tetrahydrofuran	2.90	22.5	20.0	0.5	40.0

a: Cross-sectional area; γ_L^D: surface tension; AN^*: electron acceptor number [$AN^* = 0.288(AN - AN^d)$]; DN: electron donor number.
Based on: Farinato, Kaminski, & Courter, 1990; Gutmann, 1978; Schultz et al., 1987.

temperature between 293 and 303 K. All experiments were taken at 0% RH. The experiments were done in two columns for each sample and in each replicate the probes were injected in duplicate. The results presented are the average values of four measurements. A variation less than 6% was obtained between samples columns. The experimental error between injection and due to the temperature variation, flow rate and retention time measurement was estimated to be below 4%.

2.4. IGC calculations

The net retention time of a series of homologous *n*-alkanes (dispersive) and acid-base (specific) probe molecules are used to determine the dispersive surface free energy (γ_S^D), as well as the specific free energy (ΔG_{ads}^{sp}) of adsorption, using the expression (Schultz, Lavielle, & Martin, 1987):

$$RT \quad \ln V_N = 2N_A(\gamma_S^D)^{1/2} a(\gamma_L^D)^{1/2} + \text{const.} \tag{1}$$

where V_N is the net retention volume, γ_S^D and γ_L^D the dispersive component of the surface tension of the adsorbent (i.e. the fibres) and the adsorbate, respectively, a is the cross sectional area of the adsorbate and N_A the Avogadro constant.

When polar probes are used both dispersive and specific interactions take place and thus the free energy of adsorption, ΔG_{ads}, is decomposed into two components, dispersive (ΔG_{ads}^{D}) and specific (ΔG_{ads}^{sp}):

$$\Delta G_{ads} = \Delta G_{ads}^{D} + \Delta G_{ads}^{sp} \tag{2}$$

ΔG_{ads}^{sp} corresponding to the polar (specific) probes is a measure of how easily the surface can polarize the probe. The ΔG_{ads}^{sp} data can be used to obtain the ΔH_{ads}^{sp} values (Eq. (3)) and predict surface acidity (K_a) and basicity (K_b) using the Saint-Flour and Papirer (1983) expression (Eq. (4)):

$$\frac{\Delta G_{ads}^{sp}}{T} = \Delta H_{ads}^{sp}\frac{1}{T} - \Delta S_{ads}^{sp} \tag{3}$$

$$-\frac{\Delta H_{ads}^{sp}}{AN^*} = K_a\frac{DN}{AN^*} + K_b \tag{4}$$

where DN is and AN^* are the donor and acceptor values of the polar probes, respectively. The constants K_a and K_b describe the acidity and basicity of the fibres surface, respectively.

However, the direct use of the ΔG_{ads}^{sp} (Eq. (5)) was recently suggested by Voelkel (1991) and Cava, Gavara, Lagarón, & Voelkel (2007) by rewriting the Eq. (4) in terms of ΔG_{ads}^{sp} and where K_a and K_b values were dependent on the temperature.

$$-\frac{\Delta G_{ads}^{sp}}{AN^*} = K_a\frac{DN}{AN^*} + K_b \tag{5}$$

To study the adsorption isotherm, different probe concentrations were injected (Cremer & Huber, 1962). The retention volume at the peak maximum of every injection is used to determine the monolayer capacity (Eq. (6)) and the surface area, S_{BET} (Eq. (7)), according to BET model (Brunauer, Emmet, & Teller, 1938).

$$\frac{n}{n_m} = \frac{C.x}{(1-x)[1+(C-1)x]} \tag{6}$$

$$S_{BET} = n_m \bullet a_m \bullet N_A \tag{7}$$

where n_m is the monolayer capacity, n is the adsorbed amount, C is a constant (related to the heat of adsorption), x is the reduced pressure (p/p^0), a_m the cross sectional area of a probe molecule and N_A the Avogadro constant.

In the infinite dilution region, where the isotherm is linear, V_N should be measured at a range of column temperatures and

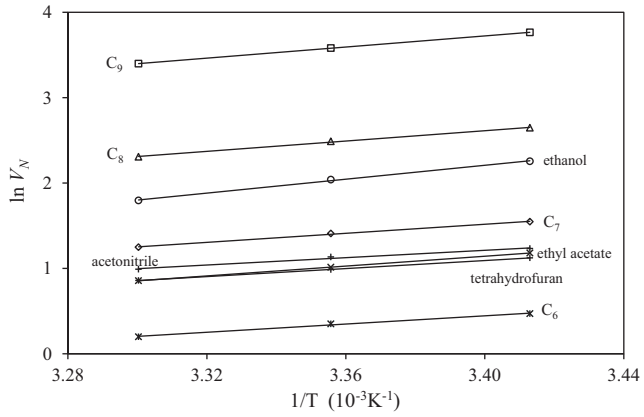

Fig. 1. Plot of ln V_N versus 1/T for *n*-alkanes and polar probes.

ln(V_N/T) plotted versus 1/T, which yields the heat of adsorption Q_{ads} according to Conder and Young (1979):

$$\left(\frac{\partial \ln\left(\frac{V_N}{T}\right)}{\partial\left(\frac{1}{T}\right)}\right) = -\frac{Q_{ads}}{R} \tag{8}$$

In addition, from the adsorption isotherm, the partial pressures can be converted into the adsorption potential (A) to determine the adsorption potential distribution according to:

$$A = RT\ln\left(\frac{p^0}{p}\right) \tag{9}$$

The first derivative of the adsorbed amount with the adsorption potential (−dn/dA) gives the distribution of surface sites of distinct energetic levels – the surface heterogeneity.

3. Results and discussion

In this work, two samples were subjected to saponin treatment: the micro and nanofibres from banana pseudo-stem. The nanofibres were obtained exposing the microfibres to a sequential steam explosion coupled with alkali treatment and acid hydrolysis (Cherian et al., 2008). This treatment provokes high changes in composition and morphology in the microfibres by the removal of the natural and artificial impurities, and lignin and non-cellulosic polysaccharides extraction. The nanofibres show high content in crystalline cellulose and small dimension (Cordeiro et al., 2012).

3.1. Dispersive surface energy

Fig. 1 shows the plot of ln V_N versus the inverse of the column temperature for *n*-alkanes and polar probes. From the values of net retention volumes (V_N) of the *n*-alkane probes, the surface properties of the fibres before and after saponin treatment are determined. The dispersive component of surface free energy γ_S^D is calculated from the ΔG_{ads}^{D} of *n*-alkanes series for every temperature. Fig. 2 shows the plots of $RT\ln V_N$ versus $a(\gamma_L^D)^{1/2}$ at different temperatures onto nanofibres before and after saponin treatment. The calculated γ_S^D values are given in Table 2, and show that the nanofibres have higher γ_S^D than the microfibres. This can be justified by the higher cellulose content, higher crystallinity and higher surface area presented by the nanofibres (Cordeiro et al., 2012). The increase in the γ_S^D can be also explained by the increase in number and in the energy of the active sites. The energetic profile (Fig. 3a) shows that the nanofibres present more energetic (A_{max} at 9.54 kJ/mol) active sites than microfibres (A_{max} at 7.15 kJ/mol).

Table 2
Dispersive component of the surface energy, γ_S^D (mJ/m^2) and acid and base surface characteristics (K_a and K_b), of the banana microfibre before and after saponin treatment.

Parameter	Banana microfibre			Saponin banana microfibre		
	293 K	298 K	303 K	293 K	298 K	303 K
γ_S^D (mJ/m^2)	41.24	39.90	39.03	48.23	46.93	45.80
K_a	0.09	0.09	0.09	0.09	0.09	0.09
K_b	0.20	0.20	0.19	0.26	0.26	0.25
K_b/K_a	2.22 (0.998)	2.22 (0.999)	2.11 (0.999)	2.89 (0.998)	2.89 (0.998)	2.78 (0.999)

Values in parenthesis are the coefficient of linear determination.

Table 3
Dispersive component of the surface energy, γ_S^D (mJ/m^2) and acid and base surface characteristics (K_a and K_b), of the banana nanofibre fibres before and after saponin treatment.

	Banana nanofibres			Saponin banana nanofibres		
	293 K	298 K	303 K	293 K	298 K	303 K
γ_S^D (mJ/m^2)	46.22	45.64	45.10	57.88	56.04	54.52
K_a	0.09	0.09	0.09	0.09	0.09	0.09
K_b	0.14	0.14	0.13	0.24	0.22	0.21
K_b/K_a	1.56 (0.997)	1.56 (0.997)	1.44(0.997)	2.67 (0.995)	2.44 (0.995)	2.33 (0.994)

Values in parenthesis are the coefficient of linear determination.

From Tables 2 and 3, it can be observed that the γ_S^D decreases linearly with the increase of temperature, that is frequently observed in lignocellulosic materials (Cordeiro et al., 2011, 2012). Banana nanofibres presented a smaller decrease in the γ_S^D with temperature, compared to the microfibres. This can be due to the higher structural organization – high crystallinity (Cherian et al., 2008) presented by these fibres, and consequently a smaller entropic dependence on the temperature than presented by micro banana fibres (Deepa et al., 2011).

The saponin treated banana fibres show characteristic peaks at 3392, 2992, 2100, 1750, 1647, 1454, 1363 and 1180 and 1100 cm^{-1} (Fig. 4). Saponin is composed of a complex skeletal ring series with preferences to chromosaponin. The stretching vibrations of the C=C bond and C=O bonds in the chromosaponin is responsible for the unique peak at 1647 cm^{-1} in saponin treated banana fibres. The intensity of this peak suggests that this group is in interaction with the surface through hydrogen bonds with the hydroxyl groups of cellulose, as schematized in Fig. 5. The methoxy group is a side chain group of the chromosaponin molecule. The stretching of the C—OH is responsible for the peak of 1113 cm^{-1}. The broad intense bands around 1180 and 1100 cm^{-1} were assigned to the stretching of the saponin—O—cellulose and saponin—O—saponin bonds, respectively. The strong increase in the intensity of these bands after the treatments suggests that the grafting of saponin onto cellulose as well as the intermolecular condensation between adjacent adsorbed chromosaponin—OH groups were substantially enhanced to get a compatible interaction for example with Poly(L-lactic acid) (PLLA). The increase of bands around 3000 cm^{-1} in saponin treated nanofibres is due to the aliphatic character of saponin's steroid body. The increase of the —OH concentration is evident from the increased intensity of the peak at 3392 cm^{-1}

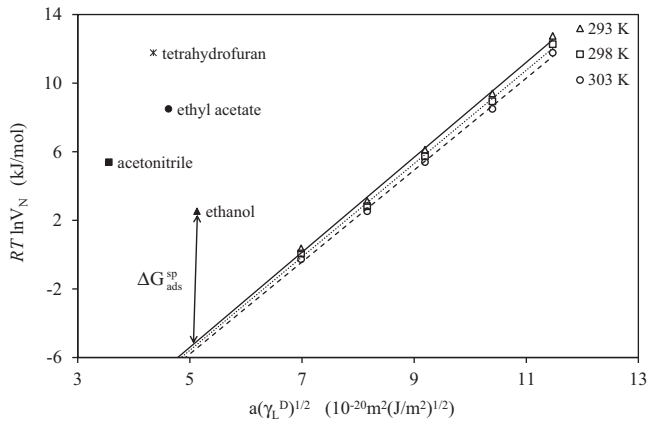

Fig. 2. Plot of $RT \ln V_N$ versus $a(\gamma_L^D)^{1/2}$ for *n*-alkanes, at different temperatures, and for polar probes (at 298 K) onto banana nanofibres.

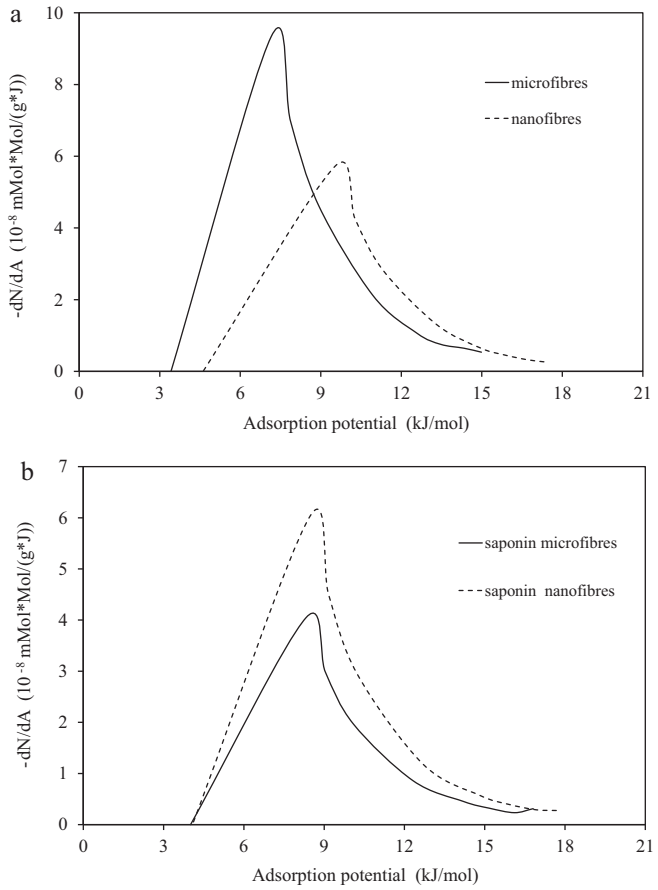

Fig. 3. Heterogeneity profiles obtained with *n*-octane onto banana micro and nanofibres before (a) and after (b) saponin, at 298 K.

Table 4
Heat of adsorption (Q_{ads}; kJ/mol) for non-polar and polar probes onto banana fibres before and after saponin treatment.

Sample	Probe (Q_{ads}, kJ/mol)				
	n-octane	Tetrahydrofuran	Ethyl acetate	Acetonitrile	Ethanol
Banana microfibre	38.94	18.33	22.54	26.79	40.36
Saponin banana microfibre	39.90	22.25	29.27	29.04	48.87
Banana nanofibre	40.17	27.11	32.46	25.14	45.25
Saponin banana nanofibres	42.90	19.63	24.14	30.21	71.68

bands of the saponin treated nanofibres compared to the untreated nanofibres. This increase in the concentration of hydroxyl density is due to the hydroxyl groups present in the chromosaponin moieties.

From Tables 2 and 3, it can be observed that γ_S^D for the surfactant coated fibres is higher compared to the untreated fibres surface: the γ_S^D for banana fibres change from 39.9 mJ/m^2 to 46.93 mJ/m^2, while the γ_S^D for nanofibres change from 45.64 to 56.04 mJ/m^2, at 298 K. The increase in γ_S^D demonstrate the effective coating of the surfactant molecules in both micro and nano fibre surfaces during the treatment process. This attachment of saponin molecules in the cellulose surface (Fig. 5) provokes an increase in the γ_S^D temperature dependence. The effect is more pronounced for nanofibers. This can suggest more saponin molecules attach the surface of this fibre compared to the microfibres. This more extended coating of the nanofibres is due to the morphologic factors (namely surface area) and to chemical surface properties (namely γ_S^D and acid/base characteristics) as discussed below.

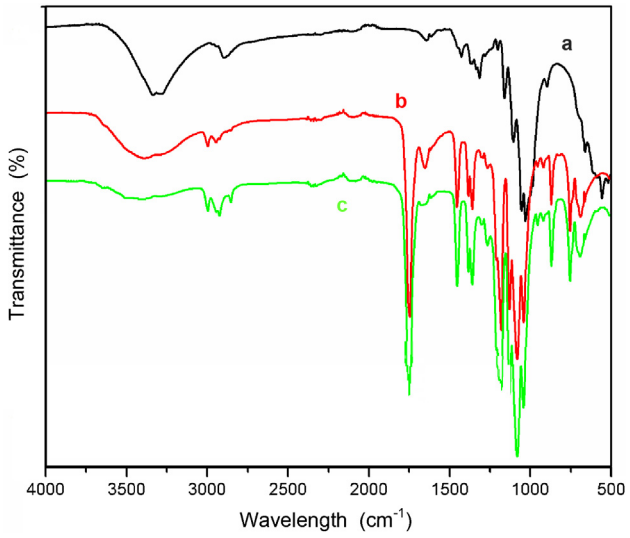

Fig. 4. FT-IR spectra of the untreated nanofibres (a), saponin treated nanofibres (b) and saponin extract (c).

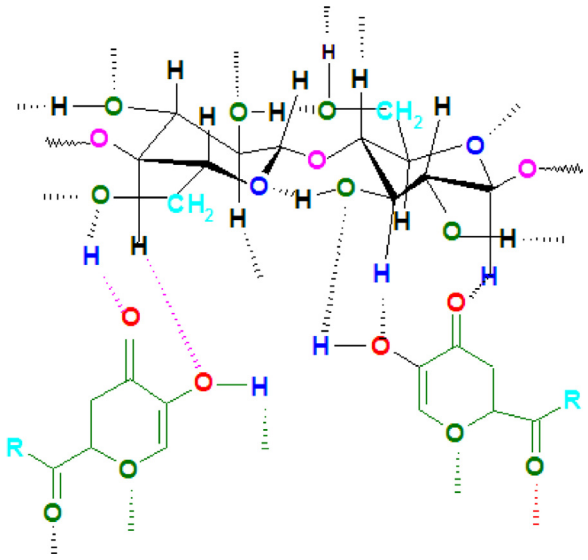

Fig. 5. Schematic representation of saponin/cellulose interaction.

The change in the dispersive component of the fibre surface can be also evaluated by heat adsorption parameter (Q_{ads}) using a non-polar probe. The Q_{ads} value obtained for the *n*-octane was 38.94 and 40.17 kJ/mol and it increased to 39.90 and 42.90 kJ/mol after saponin treatment, for micro and nanofibres, respectively (Table 4). The same tendency was observed by the calculated γ_S^D values (Tables 2 and 3). Since, as the *n*-alkane probes are able to interact only through dispersion interactions, the increase in the γ_S^D, for modified fibres, is an indication that the fibres became more hydrophobic, after saponin treatment.

Observing the energetic profiles of saponin treated fibres (Fig. 3b), and the non-treated fibres, the curves show all only a maximum (A_{max}), nevertheless, changes were detected in the intensity and in the A_{max} values. Both the coated fibres have energetic profiles at similar A_{max}, meaning that the coated fibres have the same, or similar, energetically active sites at the surface. However, the higher number of active sites presented by the nanofibres support the more extended the coating as indicated previously by the γ_S^D results.

3.2. Acid–base surface characteristics

The specific free energy of adsorption, ΔG_{ads}^{sp}, was calculated using the difference between the adsorption energy of the polar probe (acetonitrile, ethyl acetate, ethanol or tetrahydrofuran) and its dispersive increment (*n*-alkane line), as exemplified in Fig. 2. The specific interaction shows an increment in the surface interactions (below the *n*-alkanes line) indicative of acid-base groups in the fibres surface. The ΔG_{ads}^{sp} data, at 298 K, are presented in Fig. 6

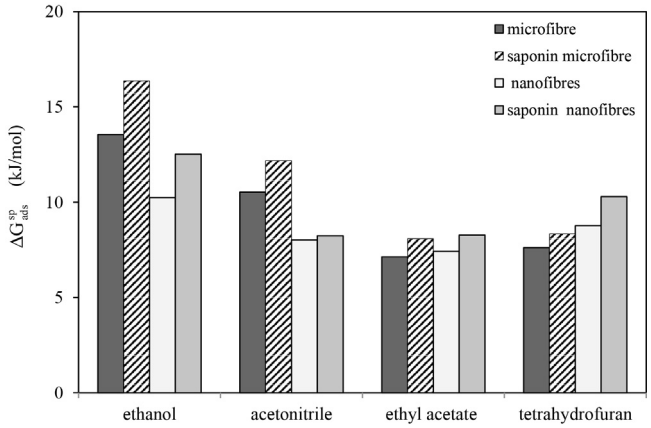

Fig. 6. Specific free energy of the adsorption for polar probes onto micro and nano banana fibres before and after saponin at 298 K.

and it shows that the calculated ΔG^{sp}_{ads} is higher for the saponin coated fibres, clearly indicating that saponin treatment creates new active sites for specific interactions in both the samples surfaces.

With the aim to study the variations in strength of the specific interaction, due to the saponin coating, the Q_{ads} was determined for the tetrahydrofuran, ethyl acetate, acetonitrile and ethanol probes, at 293, 298 and 303 K. Good linearity was obtained (correlation coefficient >0.98) and the respective values for Q_{ads} are resumed in Table 4. The greater increase (58.9%) in Q_{ads} values for ethanol (lower DN/AN*) suggest that the saponin treatment significantly increased the basicity of the nanofibres surface. In the case of saponin banana nanofibres, the decrease in Q_{ads} for the acidic probe, tetrahydrofuran (higher DN/AN*), suggests a decrease in acidity of the nanofibre surface. As illustrated in Fig. 5, the oxygenated groups in the saponin molecules create hydrogen bonds with the acidic groups in the cellulose polymers. To an extensive coating a network was formed and was expected a decrease in the free acid groups in the fibres surface. On the other hand, due to the higher number of the basic groups in the saponin molecules, the total of basic sites increase in the new coated surface. In the case of the microfibres the Q_{ads} increased for all the probes. This suggests a coating process less extensive to these fibres without an extended network formation, which leaves free some of the saponin acid and basic groups, increased the active sites number which contribute to the Q_{ads}, increasing.

As referred in Section 2.5, the calculated ΔG^{sp}_{ads} was used to predict surface acidity (K_a) and basicity (K_b), by two processes, directly (Eq. (5)) or through the calculation of ΔH^{sp}_{ads} (Eq. (4)). In both cases, a linear fitting of the correlation coefficient shows that the Gutmann's acid–base concept is valid for the studied samples and that the specific interactions may be considered of the electron donor–acceptor type.

Using directly the ΔG^{sp}_{ads} data (Eq. (5)), the calculated K_a and K_b (Tables 2 and 3) show the predominant basicity characteristics of the fibre surface for the different temperatures. The K_b values were found to increase with the saponin treatment for both fibres (micro and nanofibres). However, the K_b/K_a ratio values increase more significantly for the nanofibres (from 1.56 to 2.44, at 298 K) (56.4%) than for the banana microfibres (from 2.22 to 2.89, at 298 K) (30.2%), reinforcing the previous conclusions of a more extended coating on the nanofibres surface.

The calculated K_a and K_b are presented in Table 5 and show clearly that all fibres (before and after treatment) have a predominant Lewis basic surface, with weak acidity. The increase in basic character due to surfactant coating is in good agreement with the higher ΔG^{sp}_{ads} and Q_{ads} for the polar probes with lower DN/AN* (major donor capacity) when compared to the untreated fibres. The reasons behind the increase in basic character of the fibres surface due to saponin treatment can be explained only on the composition of saponin used in the present study. The basicity comes from its oxygen groups. Therefore, the saponin modified fibres tend to adsorb acidic molecules.

Table 5
Acid and base surface characteristics (K_a and K_b) of the banana fibres before and after saponin treatment.

Sample	K_a	K_b	K_b/K_a	Coefficient of determination
Banana microfibre	0.09	0.65	7.2	0.97
Saponin banana microfibre	0.08	0.69	8.6	0.98
Banana nanofibre	0.11	0.53	4.8	0.96
Saponin banana nanofibres	0.07	1.15	16.4	0.99

Table 6
Adsorption potential distribution maximum (A_{max}), specific surface area (S_{BET}) and monolayer capacity (n_m), at 298 K, for the banana fibres before and after saponin treatment.

Sample	A_{max} (kJ/mol)	S_{BET} (m^2/g)	n_m (μMol/g)
Banana microfibre	7.15	0.492	1.30
Saponin banana microfibre	8.32	0.189	0.497
Banana nanofibre	9.54	1.342	3.54
Saponin banana nanofibres	8.45	0.358	0.942

The determination of K_a and K_b using the ΔG^{sp}_{ads} directly (Eq. (5)) leads to temperature dependent values containing also entropic factor. This value will be similar to the K_a and K_b calculated through ΔH^{sp}_{ads} (Eq. (4)), if the entropic contribution can be assumed to be negligible. In the present study, the K_a and K_b show that they are greatly influenced by temperature.

3.3. Isotherm measurements

Considering the morphological aspect, Scanning Electron Microscope analysis of saponin treated micro and nanofibres (Fig. 7) showed differences in the degree of modification and morphology of the cellulose fibres as discussed by Cherian et al. (2012).

The IGC analysis shows that the nanofibres have a very high surface area – S_{BET} – and monolayer capacity – n_m (1.342 m^2/g and 3.45 μMol/g) compared to the microfibres (0.492 m^2/g and 1.30 μMol/g). These aspects coupled with the higher γ^D_S, Q_{ads} and the acidic character of the nanofibres, explain the more reactive surface and consequently the more extensive saponin coating for the nanofibres compared to the microfibres.

The reaction between the fibres and the saponin is reported by the substantial decrease in S_{BET} (Table 6), with a reduction of 61% to microfibres and 73% to the nanofibres. The significant increase in

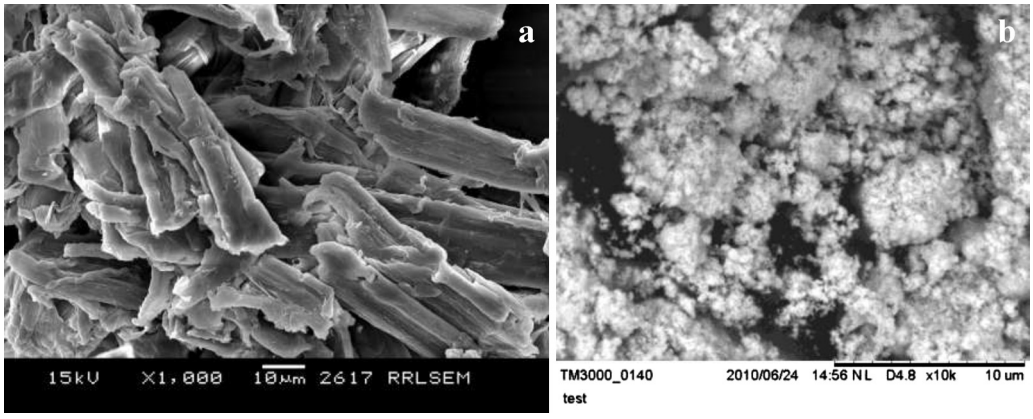

Fig. 7. Scanning electron micrographs taken from the macrofibres (a) and saponin treated nanofibres (b).

the particle size could be justified by the high coating with saponin molecules, with a network formation.

4. Conclusions

Banana cellulose micro and nanofibres obtained by steam explosion process were soaked with saponin, a surfactant extracted from soapnut fruit. A comprehensive insight into the dispersive and Lewis acid–base surface interactions studied by inverse gas chromatography provides a better understanding about the influence of the chemical modification of the fibres, as well as their ability to change via chemical modifications with respect to the nanometre dimension, which is of great importance for their applications. The saponin treatment with micro and nanofibres showed differences in the degree of modification and morphology of the cellulose fibres. The results clearly show that the saponin can provide a continuous path of hydrogen bonds between the fibre surfaces which will thus enhance the hydrophobic and the acid–base nature of the fibre surface. This behaviour will lead to better polymer/fibre interaction during the composite preparation.

Acknowledgements

Portuguese authors would like to thank the "*Programa Nacional de Re-equipamento Científico*", POCI 2010, for sponsoring IGC work (FEDER and Foundation for the Science and Technology). Indian authors thank the Department of Science and Technology, New Delhi, for financial support for the project.

References

Abraham, E., Deepa, B., Pothan, L. A., Jacob, M., Thomas, S., Cvelbar, U., et al. (2011). Extraction of nanocellulose fibrils from lignocellulosic fibres: A novel approach. *Carbohydrate Polymers*, *86*, 1468–1475.

Belgacem, M. N., Salon-Brochier, M. C., Krouit, M., & Bras, J. (2011). Recent advances in surface chemical modification of cellulose fibres. *Journal of Adhesion Science and Technology*, *25*, 661–684.

Brunauer, S., Emmet, P. H., & Teller, E. (1938). Adsorption of gases in multimolecular layers. *Journal of the American Chemical Society*, *60*, 309–319.

Böttger, S., Hofmann, K., & Melzig, M. F. (2012). Saponins can perturb biologic membranes and reduce the surface tension of aqueous solutions: A correlation? *Bioorganic & Medicinal Chemistry*, *20*, 2822–2828.

Cava, D., Gavara, R., Lagarón, J. M., & Voelkel, A. (2007). Surface characterization of poly(lactic acid) and polycaprolactone by inverse gas chromatography. *Journal of Chromatography A*, *1148*, 86–91.

Cherian, B. M., Pothan, L. A., Nguyen-Chung, T., Mennig, G., Kottaisamy, M., & Thomas, S. (2008). Novel method for the synthesis of cellulose nanofibril whiskers from banana fibers and characterization. *Journal of Agricultural and Food Chemistry*, *56*, 5617–5627.

Cherian, B. M., Leão, A. L., Caldeira, M. S., Chiarelli, D., Souza, S. F., Narine, S., et al. (2012). Use of saponins as an effective surface modifier in cellulose nanocomposites. *Molecular Crystals and Liquid Crystals*, *556*, 233–245.

Conder, J., & Young, C. (1979). *Physicochemical measurement by Gas Chromatography*. Chichester: John Wiley & Sons Ltd.

Cordeiro, N., Gouveia, C., & John, M. J. (2011). Investigation of surface properties of physico-chemically modified natural fibres using inverse gas chromatography. *Industrial Crops and Products*, *33*, 108–115.

Cordeiro, N., Mendonça, C., Pothan, L. A., & Varma, A. (2012). Monitoring surface properties evolution of thermochemically modified cellulose nanofibres from banana pseudo-stem. *Carbohydrate Polymers*, *88*, 125–131.

Cremer, E., & Huber, H. (1962). Measurement of adsorption isotherms by means of high temperature elution gas chromatography. *International Symposium on Capillary Chromatography*, *3*, 169–182.

Deepa, B., Abraham, E., Cherian, B. M., Bismarck, A., Blaker, J. J., Pothan, L. A., et al. (2011). Structure, morphology and thermal characteristics of banana nano fibers obtained by steam explosion. *Bioresource Technology*, *102*, 1988–1997.

Eichhorn, S. J., Baillie, C. A., Zafeiropoulos, N., Mwaikambo, L. Y., Ansell, M. P., Dufresne, A., et al. (2001). Review: Current international research into cellulosic fibres and composites. *Journal of Materials Science*, *36*(9), 2107–2131.

Farinato, R. S., Kaminski, S. S., & Courter, J. L. (1990). Acid-base character of carbon-fiber surfaces. *Journal of Adhesion Science and Technology*, *4*, 633–652.

Gutmann, V. (1978). *The Donor-Acceptor Approach to Molecular Interactions*. New York: Plenum Publ. Corp.

Guglu-Ustundag, O., & Mazza, G. (2007). Saponins: Properties, applications and processing. *Critical Reviews in Food Science and Nutrition*, *47*, 231–258.

Habibi, Y., Lucia, A. L., & Rojas, O. J. (2010). Cellulose Nanocrystals: Chemistry, Self-Assembly, and Applications. *Chemical Reviews*, *110*, 3479–3500.

Lu, J., Askeland, P., & Drzal, L. T. (2008). Surface modification of microfibrillated cellulose for epoxy composite applications. *Polymer*, *49*, 1285–1296.

Mohanty, A. K., Misra, M., & Hinrichsen, G. (2000). Biofibers, biodegradable polymers and biocomposites: An Overview. *Macromolecular Materials and Engineering*, *276-277*, 1–24.

Oliveira, L., Cordeiro, N., Evtuguin, D. V., Torres, I. C., & Silvestre, A. J. D. (2007). Chemical composition of different morphological parts from 'Dwarf Cavendish' banana plant and their potential as a non-wood renewable source of natural products. *Industrial Crops and Products*, *26*, 163–172.

Saint-Flour, C., & Papirer, E. (1983). Gas-solid chromatography: a quick method of estimating surface free energy variations induced by the treatment of short glass fibers. *Journal of Colloid and Interface Science*, *91*, 69–75.

Schultz, J., Lavielle, L., & Martin, C. (1987). The role of the interface in carbon fiber/Epoxy composites. *Journal of Adhesion*, *23*, 45–60.

Rao, A. S. V. S., Basa, S. C., & Srinivasulu, C. (1992). Improved process for the production of saponin from soapnuts. *Research and Industry*, *37*, 209–210.

Tsurumi, S., Ishizawa, K., Rahman, A., Soga, K., Hoson, T., Goto, N., et al. (2000). Effects of chromosaponin I and brassinolide on the growth of roots in etiolated arabidopsis seedlings. *Journal of Plant Physiology*, *156*, 60–67.

Tze, W. T. Y., Wålinder, M. E. P., & Gardner, D. J. (2006). Inverse gas chromatography for studying interaction of materials used for cellulose fiber/polymer composites. *Journal of Adhesion Science and Technology*, *20*, 743–759.

Voelkel, A. (1991). Inverse gas chromatography: Characterization of polymers, fibers, modified silicas and surfactants. *Critical Reviews in Analytical Chemistry*, *22*, 411–439.